

Disruption of Functional Networks in Dyslexia: A Whole-Brain, Data-Driven Analysis of Connectivity

Emily S. Finn, Xilin Shen, John M. Holahan, Dustin Scheinost, Cheryl Lacadie, Xenophon Papademetris, Sally E. Shaywitz, Bennett A. Shaywitz, and R. Todd Constable

Background: Functional connectivity analyses of functional magnetic resonance imaging data are a powerful tool for characterizing brain networks and how they are disrupted in neural disorders. However, many such analyses examine only one or a small number of a priori seed regions. Studies that consider the whole brain frequently rely on anatomic atlases to define network nodes, which might result in mixing distinct activation timecourses within a single node. Here, we improve upon previous methods by using a data-driven brain parcellation to compare connectivity profiles of dyslexic (DYS) versus nonimpaired (NI) readers in the first whole-brain functional connectivity analysis of dyslexia.

Methods: Whole-brain connectivity was assessed in children ($n = 75$; 43 NI, 32 DYS) and adult ($n = 104$; 64 NI, 40 DYS) readers.

Results: Compared to NI readers, DYS readers showed divergent connectivity within the visual pathway and between visual association areas and prefrontal attention areas; increased right-hemisphere connectivity; reduced connectivity in the visual word-form area (part of the left fusiform gyrus specialized for printed words); and persistent connectivity to anterior language regions around the inferior frontal gyrus.

Conclusions: Together, findings suggest that NI readers are better able to integrate visual information and modulate their attention to visual stimuli, allowing them to recognize words on the basis of their visual properties, whereas DYS readers recruit altered reading circuits and rely on laborious phonology-based “sounding out” strategies into adulthood. These results deepen our understanding of the neural basis of dyslexia and highlight the importance of synchrony between diverse brain regions for successful reading.

Key Words: Brain networks, dyslexia, fMRI, functional connectivity, reading, visual attention

Developmental dyslexia, or specific reading disability, is defined as an unexpected difficulty in accuracy or fluency of reading for the age, intelligence, level of education, or professional status of an individual (1). It is the most commonly diagnosed learning disability in the United States, with prevalence estimates ranging from 5% to 17.5% (2–4).

Functional magnetic resonance imaging (fMRI) studies have largely converged on three left-hemisphere brain areas whose activity is altered in dyslexia (5–7). These are: 1) a parietotemporal region; 2) the inferior frontal gyrus (IFG); and 3) an occipitotemporal region, including the visual word-form area (VWFA), part of the fusiform gyrus that is seemingly responsible for rapid word recognition (8–12). These areas and their right-hemisphere homologs show over- or underactivation to reading tasks in dyslexic relative to nonimpaired readers, in both children and adults (5,13–16).

However, activation-based analyses of fMRI data do not address how brain regions interact and therefore might give an incomplete picture of the neural underpinnings of dyslexia. Functional connectivity analyses can detect differences in areas with similar magnitudes of activation but whose activity is

differentially synchronized with other areas across subject groups and/or types of stimuli. This synchrony between anatomically distinct regions might be equally or more important for cognitive performance than the magnitude of activation in any single region (17).

Although there have been some functional connectivity studies of dyslexia (18–22), all of these have examined connections between specific regions chosen a priori. These regions follow the literature of task-based results and represent only a small fraction of the brain. Previous studies, then, potentially fail to provide a complete picture of the connectivity profiles of dyslexic versus nonimpaired readers.

In this article we present, to our knowledge, the first whole-brain functional connectivity study of dyslexia. Connectivity was examined in two large datasets of children and young adults. We used a novel method for parcellating voxels into functional subunits to use as nodes (23,24) and contrasted the connection strengths—defined as correlations between signal timecourses—between dyslexic (DYS) and nonimpaired (NI) readers for all possible pairs of nodes to determine networks that are differentially connected across reading groups.

We hypothesized that these data-driven methods would reveal differences in previously characterized areas but also in new, less well-characterized networks, thereby revealing the functional brain networks that crucially support the complex cognitive task of reading.

Methods and Materials

Participants

All data were acquired with written consent of participants and in accordance with the Institutional Review Board of Yale University. Data are from two previously unpublished sets of DYS readers and NI control subjects. Participants were classified as dyslexic on the basis of sub-25th percentile performance on one

From the Interdepartmental Neuroscience Program (ESF); Yale Center for Dyslexia and Creativity (JMH, SES, BAS); Department of Biomedical Engineering (DS, XP, RTC), Yale University; Department of Diagnostic Radiology (XS, CL, XP, RTC); and the Department of Neurosurgery (RTC), Yale University School of Medicine, New Haven, Connecticut.

Address correspondence to Emily S. Finn, B.A., Yale University, Interdepartmental Neuroscience Program, 300 Cedar Street, PO Box 208043, New Haven, CT 06520-8043; E-mail: emily.finn@yale.edu.

Received Apr 2, 2013; revised Aug 19, 2013; accepted Aug 27, 2013.

of the following batteries: 1) the Gray Oral Reading Test-IV (GORT) (25) Fluency score (the composite of rate and accuracy); 2) either GORT subtest score (rate or accuracy); or 3) the Test of Word Reading Efficiency (26) total score, combined with a sub-25th percentile score on the Woodcock-Johnson battery (27). The NI readers scored above the 25th percentile on all GORT, Woodcock-Johnson, and Test of Word Reading Efficiency measures.

The first dataset contained 80 children (“young readers,” mean age 8.9 years); the second contained 104 young adults (“older readers,” 64 NI, 40 DYS; mean age 20.8 years). After applying exclusion criteria to ensure there were no significant differences in head motion between groups (Supplement 1), 75 young readers (43 NI, 32 DYS) were entered into the final analysis.

Participant demographic and behavioral data are shown in Table 1. All participants were right-handed. Dyslexia and attention disorders are highly comorbid (28); although data on attention measures and attention-deficit disorder or attention-deficit/hyperactivity disorder status of participants were not explicitly collected, none were on a regimen of psychoactive medication at the time of scanning. The NI and DYS participants differed significantly on all behavioral reading measures ($p < .001$). Groups did not differ significantly in age ($p > .05$). There was a significant relationship between sex and group in young readers, with the proportion of male subjects higher in the DYS group (Cochran-Mantel-Haenszel χ^2 test: $\chi^2 = 6.27$, $p = .01$). There was no difference in sex breakdown in older participants ($\chi^2 = .71$, $p = .4$). Although IQ scores (29) were higher in the NI group, all DYS participants had normal-range IQ scores; it is difficult to balance groups along this dimension, because reading ability and cognition are strongly linked (30). Still, studies have found that the presence or absence of reading disability is a better predictor of performance than IQ scores on tasks involving reading and related behaviors (31). To control for the observation that IQ was lower in the DYS group, we performed ancillary analyses in a subset of the cohort matched for performance IQ; see Supplement 1 for a description of these analyses and their results. Results from these IQ-matched subsets were highly consistent

with the original analyses; thus data from the full cohort are presented here.

Each subject underwent four functional runs while performing a word- and non-word-rhyming task. The effect of task was regressed out for purposes of the connectivity analysis (Supplement 1). Regressing out activation associated with task leaves residual fluctuations that more closely represent intrinsic, spontaneous neural activity (32). In using residuals, we avoid our results being dominated by activation coupled to the processing of each stimulus and instead examine fluctuations that occur independently of individual task stimuli. Although overall brain state during task performance could subtly affect these fluctuations, in the case of dyslexia—a disorder with the specific task of reading—these effects might serve to enhance the contrast in functional organization between groups. See Supplement 1 for MRI acquisition parameters, information about task regression, and other preprocessing steps.

Connectivity Analysis Pipeline

Analysis consisted of the following steps: 1) defining network nodes with a novel whole-brain parcellation; 2) calculating connectivity matrices for each subject; 3) comparing matrices to identify significant group differences in correlation strength; and 4) correcting for multiple comparisons with the network-based statistic (NBS) (33). See Figure 1 for a schematic of this analysis.

Defining Network Nodes. A major consideration in functional connectivity analyses is how to delineate brain regions to use as nodes. Especially in the cortex, where structural boundaries are often unclear, choices such as how to draw node boundaries and how many nodes to include can greatly impact the properties—and neurobiological validity—of the resulting network (34).

Previous studies have commonly defined nodes in one of four ways: 1) anatomically, with the Brodmann-based automatic anatomic labeling atlas (35–39); 2) functionally, according to task data from the same or previous fMRI studies (40,41) (but note this approach provides limited brain coverage, depending on which areas activated to the task[s]); 3) by treating each individual voxel

Table 1. Participant Demographic and Behavioral Data

	Young Readers						Older Readers					
	DYS, $n = 32$			NI, $n = 43$			DYS, $n = 40$			NI, $n = 64$		
	Mean	(z)	SD	Mean	(z)	SD	Mean	(z)	SD	Mean	(z)	SD
Age	9.13		1.03	8.69		1.16	20.83		2.99	19.72		3.06
WASI IQ: Full Scale	98.7	-.09	13.6	122.5	1.50	13.9	102.6	.17	13.0	114.9	.99	11.2
WASI IQ: Verbal	102.4	.16	12.4	125.7	1.71	11.6	102.0	.13	14.5	115.5	1.03	12.6
WASI IQ: Performance	95.5	-.30	13.7	115.0	1.00	17.2	101.7	.12	14.7	110.5	.70	11.7
WJ: Word ID	86.4	-.90	5.9	121.8	1.45	10.8	83.7	-1.09	8.6	109.3	.62	9.5
WJ: Word Attack ^a	88.1	-.79	5.7	114.2	.95	9.9	78.4	-1.44	7.4	101.2	.08	6.9
TOWRE: Word Reading	84.9	-1.01	11.0	118.9	1.26	9.9	78.4	-1.44	8.0	99.1	-.06	12.2
TOWRE: Phonologic Decoding ^a	81.1	-1.26	5.7	114.1	.94	10.0	68.8	-2.08	8.1	98.8	-.08	8.3
GORT: Rate	5.50	-1.50	2.05	14.02	1.34	2.05	5.23	-1.59	1.66	11.98	.66	1.39
GORT: Accuracy	4.28	-1.91	1.89	12.14	.71	2.82	3.73	-2.09	2.16	12.91	.97	1.98
GORT: Fluency	4.28	-1.91	1.76	13.28	1.09	2.54	2.40	-2.53	1.53	14.08	1.36	2.16
GORT: Comprehension	8.31	-.56	3.27	13.33	1.11	3.11	7.78	-.74	2.33	10.45	.15	1.97
Gender (n)												
M	22			17			24			33		
F	10			26			16			31		

The IQ, Woodcock-Johnson (WJ) (25), and Test of Word Reading Efficiency (TOWRE) (24) measures are given in standard scores normalized to mean 100, SD 15; Gray Oral Reading Test IV (GORT) (23) measures are standard scores normalized to mean 10, SD 3. Groups differed significantly at $p < .001$ on all listed behavioral measures (IQ, WJ, TOWRE and GORT).

DYS, dyslexic; NI, nonimpaired; WASI, Wechsler Abbreviated Scale of Intelligence (26).

^aTest uses non-words (pseudowords).

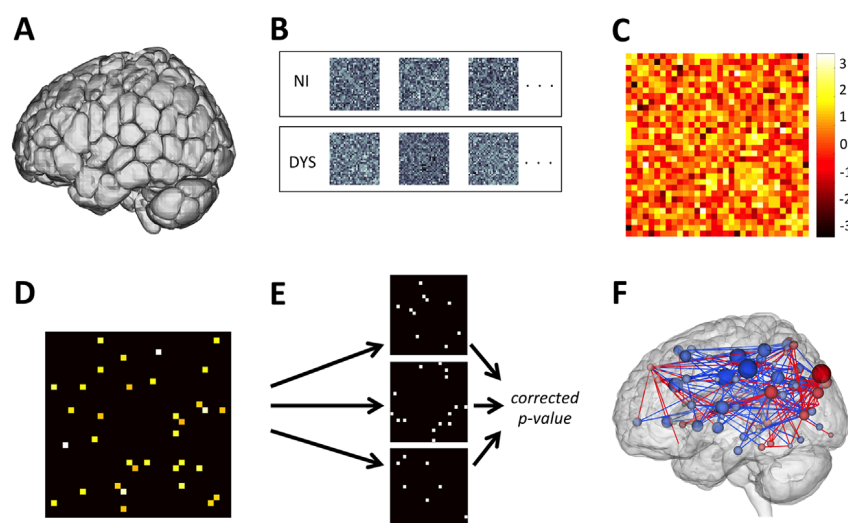


Figure 1. Schematic of connectivity analysis. Steps in the present approach to connectivity analysis: **(A)** use groupwise parcellation algorithm (24) to divide whole brain into n (approximately 200) nodes by grouping voxels with maximally similar timecourses; **(B)** calculate $n \times n$ connectivity matrices of normalized correlation values for each possible pair of nodes for each subject; **(C)** perform two-tailed t test on each cell of the matrix; **(D)** threshold on the basis of chosen t score, calculate largest connected component of suprathreshold edges in each direction (nonimpaired readers [NI] > dyslexic readers [DYS] and $DYS > NI$); **(E)** correct for multiple comparisons by randomly permuting group assignment and recalculating largest connected component size to create a null distribution for expected component size due to chance; and **(F)** visualize any components surviving correction.

as a node (42,43); or 4) using algorithms independent of anatomy or function that divide the brain into arbitrarily defined regions (44).

With the exception of the voxel-based approach, the problem with these parcellation schemes is the potential to mix activation timecourses within a single node, resulting in an average timecourse that does not accurately represent any of the individual voxels within. Such flawed averaging could render meaningless results. In the present study, we used a novel groupwise parcellation method to divide the brain into regions optimized to contain voxels with similar temporal signal fluctuations (23,24). This purely data-driven approach yields nodes with more coherent timecourses than nodes defined with the automatic anatomic labeling atlas, even at the same whole-brain resolution (24). See Figure 1A for an example of a whole-brain functional parcellation.

Because the brain undergoes significant changes between childhood and young adulthood, we parcellated young and older readers separately to delineate nodes that were maximally functionally coherent within each age group. For younger readers, 20 parcellations were generated from randomly selected groups of 30 NI participants, and the parcellation with the best whole-brain reproducibility score was selected and applied to all participants. For older readers, the best parcellation was chosen from 20 parcellations generated from randomly selected groups of 45 NI participants.

This process resulted in parcellations of 205 nodes for young readers and 207 nodes for older readers. The parcellations, defined in standard space, were warped to subject space with the transformation from a subject's three-dimensional anatomical image to the Montreal Neurological Institute brain (45). Although parcellations were defined using data from NI participants, there was no difference in whole-brain inhomogeneity scores between the NI and DYS groups ($p = .30$ in young readers, $p = .26$ in older readers). Inhomogeneity is defined as the Euclidean distance between the timecourse of an individual voxel and the mean timecourse of the node to which it belongs; the whole-brain homogeneity index for an individual subject is calculated by summing Euclidean distances for all voxels (24).

Computing Connectivity Matrices. With the respective group parcellation (younger or older), for each subject we computed the pairwise correlation coefficient between the timecourses of each possible pair of nodes with data from all runs from that subject. The R values were normalized to Z scores with the Fisher

transformation, resulting in a 205×205 symmetric connectivity matrix for each young participant and a 207×207 matrix for each older participant. Each cell of the matrix represents the strength of the connection, or "edge," between two particular nodes.

Computing Edge-Wise Differences. With the individual-subject matrices as inputs, we performed a two-tailed t test on the values of each cell to create a "difference matrix" of t scores representing the magnitude of group difference at each edge (Figure 1C). We then thresholded this matrix for statistical significance at $p < .01$ (Figure 1D). Calculations described in the next section were performed on the left and right tails separately such that direction of differences could be identified (i.e., $NI > DYS$ or $DYS > NI$).

Multiple-Comparison Correction. To correct for multiple comparisons, we used the NBS (33). This method, analogous to cluster correction for graphs, provides a solution to the statistical problem of massively multiple comparisons in a whole-brain connectivity analysis. In the NBS, with the difference matrix as the input (see preceding subsection text), the largest fully connected network of suprathreshold edges, or "component," is identified, and its extent is defined as the number of edges it comprises. Finally, these calculations are repeated for a large number of trials in which the group assignments of subjects are randomly permuted to create a null distribution for the expected component size due to chance (Figure 1E).

Group Data Analyses. We performed the aforementioned analysis to compare connectivity between the NI and DYS groups in both datasets ($\alpha = .01$; young readers: t threshold = ± 2.645 ($df = 73$); older readers, t threshold = ± 2.625 ($df = 102$); both groups, $K = 5000$ randomizations in the NBS step).

Results

Young Readers

In young readers, we identified two differentially connected networks: one more strongly connected in the NI group (component size = 337 edges; $p < .01$, corrected) and one more strongly connected in the DYS group (component size = 415; $p < .01$, corrected). The full $NI > DYS$ (red) and $DYS > NI$ (blue) networks are shown in Figure S1A in Supplement 1. We refer to the $NI > DYS$ network as simply the "NI" network, and the $DYS > NI$ network as the "DYS" network.

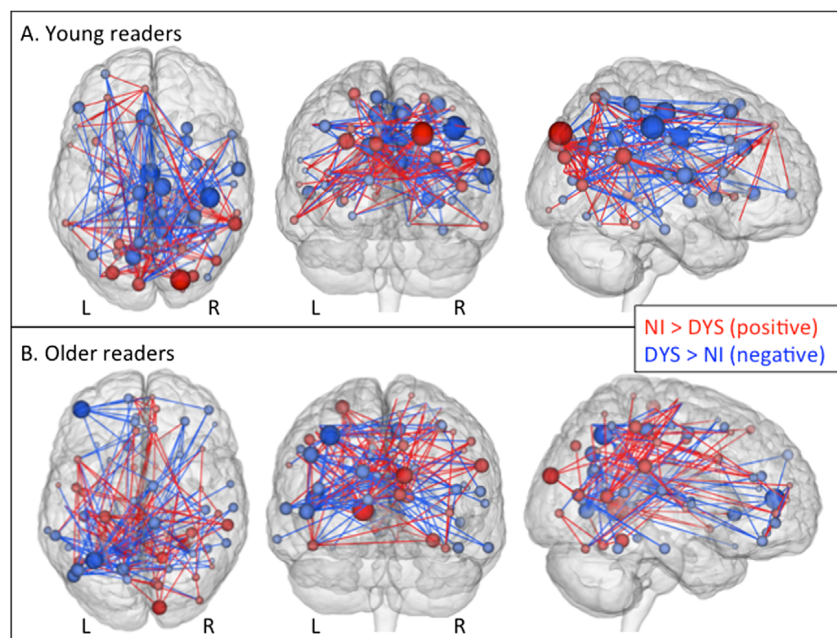


Figure 2. Whole-brain connectivity differences between groups. Three-dimensional representation of the non-impaired readers (NI) > dyslexic readers (DYS) (“NI”) and DYS > NI (“DYS”) edge components ($p < .01$ after network-based statistic correction) in young readers (A) and older readers (B). Red lines denote the NI network; blue lines denote the DYS network. These components were thresholded for scarcity to show nodes with a sum of edges differences ≥ 15 in younger readers and ≥ 10 in older readers along with all the nodes to which these suprathreshold nodes were connected, representing approximately 1% of the total number of edges in both age groups. Spheres are placed at the centroid of each node and are scaled and colored according to their numbers of edges in the NI and DYS networks (i.e., large red nodes have many more NI edges than DYS edges, and vice versa for large blue nodes). Note that all figures are shown in neurological convention (subject-left is image-left): axial views are top-down, and coronal views are from the posterior. L, left; R, right.

Although the components that survived correction at $p < .01$ represented only approximately 3% of the total edges in the brain, this number is sufficiently large to make visualization of all edges challenging. To focus our analysis on regions where connectivity was maximally different between groups, we further reduced these figures to include only those nodes with a “sum of edge differences” of at least 15 as well as their functional partners (Figure 2A; see Table 2 for a list of these six nodes and their coordinates; see Table S1 in Supplement 1 for a list of coordinates of all functional partners for each selected node). The sum of edge differences of a node was defined as the sum of its edges in both the NI and DYS networks (i.e., its total number of differential connections). The advantage of this method is the ability to detect nodes with the similar numbers of edges but different functional partners in each network. For example, node D in younger readers had eight edges in both the NI and DYS networks, so in a standard degree measurement its difference would be zero (Table 2). However, preserving information about the location of connections and calculating the sum of edge differences—16 in this case—reveals this node as a locus of significant divergence between groups.

Individual nodes were selected for discussion in the following manner. We visualized the connectivity profiles of the top four nodes with the highest sum of edge differences (at least 16), along with their functional partners in both the NI and DYS networks, in Figure 3 (panels A, B, C, and D). In addition, we reasoned that nodes with very strong directionality (i.e., those with all NI > DYS or all DYS > NI edges) were also important loci of network differences. Thus we also profiled the two nodes with the highest difference of edges (Figure 3E, 14 NI/0 DYS edges; Figure 3F, 0 NI/14 DYS edges). See Figure S2 and Table S4 in Supplement 1 for node-level results from the IQ-matched subset.

Older Readers

In older readers, we identified an NI > DYS network (component size = 312 edges; $p < .01$, corrected) and a DYS > NI network (component size = 361 edges; $p < .01$, corrected), referred to as the “NI” and “DYS” networks, respectively. Full networks are shown in Figure S1B in Supplement 1. As with results from younger readers, for visualization purposes, we further reduced these figures to show nodes with a sum of edge differences of at least 10 (Figure 2B; see Table 3 for coordinates of

Table 2. Node-Level Analysis in Younger Readers

Node	Region	Talairach	NI > DYS Edges	DYS > NI Edges	Sum of Edges	Diff of Edges
Nodes with a Sum of Edge Differences of at Least 15 ^a :						
A ^b	L sup cuneus (BA19)	(−9, −84, 30)	12	6	18	6
B ^b	L/R pCC (BA23)	(6, −41, 21)	4	13	17	−9
C ^b	L mFG (BA8)	(−5, 44, 37)	9	7	16	2
D ^b	R calc. (BA17/23)	(11, −71, 11)	8	8	16	0
G	R sTG/SMG (BA39/40)	(58, −45, 23)	11	4	15	7
H	L/R cing (BA23)	(0, −12, 32)	1	14	15	−13
Nodes with all One-Sided Edge Differences:						
E ^b	R sup cuneus (BA19)	(21, −81, 35)	14	0	14	14
F ^b	R SMG (BA40)	(41, −27, 38)	0	14	14	−14

BA, Brodmann area; calc., calcarine sulcus; cing, cingulate cortex; diff, difference; DYS, dyslexic; L, left; mFG, medial frontal gyrus; NI, nonimpaired; pCC, posterior cingulate cortex; R, right; SMG, supramarginal gyrus; sTG, superior temporal gyrus; sup, superior.

^aShown in Figure 2A.

^bShown in Figure 3.

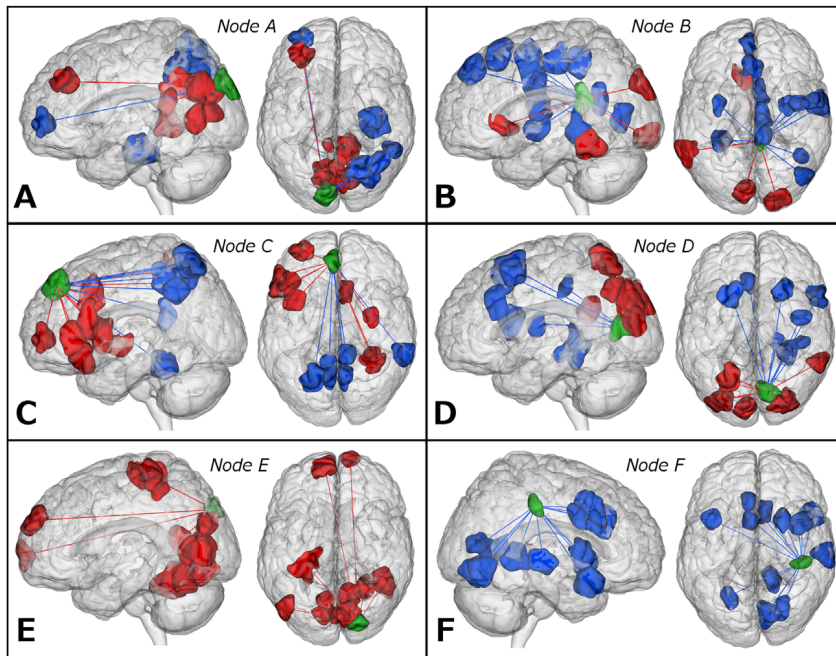


Figure 3. Visualization of connectivity profiles of selected nodes in young readers. We display the connectivity profile of the six nodes with maximal group differences in connectivity (of a total of 205 nodes; see Results section 1 for how these nodes were selected). In each case the selected node is shown in green (see Table 2 for the coordinates of each selected node), whereas nodes more strongly connected to the selected node in the nonimpaired readers (NI) > dyslexic readers (DYS) (“NI” network are shown in red, and nodes more strongly connected to the selected node in the DYS > NI (“DYS”) network are shown in blue (see Table S1 in Supplement 1 for the coordinates of all NI and DYS partner nodes). Red and blue lines simply schematize connectivity between the selected node and each of its functional partners. Approximate anatomical locations of selected nodes: (A) left superior cuneus (Brodmann area [BA] 19); (B) posterior cingulate cortex; (C) left medial frontal gyrus (BA 8); (D) right calcarine sulcus (BA 17/23); (E) right superior cuneus (BA 19); and (F) right supra-marginal gyrus (BA 40). Note that all figures are shown in neurological convention: subject-left is image-left, and axial views are top-down.

each selected node; see Table S2 in Supplement 1 for a list of coordinates of all functional partners for each selected node).

To identify nodes for further discussion, we chose the node with the highest sum of edge differences (node J; Figure 4A) as well as a node with entirely DYS > NI connections (node Q; Figure 4B). Given the prominence of the VWFA in the dyslexia neuroimaging literature, we also show the connectivity profile of the node in the parcellation corresponding to the VWFA (node R, Figure 4C; defined on the basis of the Talairach coordinates for peak activation in the VWFA as reported in two recent seed-based connectivity studies of dyslexia [(20): (−40, −55, −10); (21): (−43, −62, −1); center of mass for parcellation node R (−42, −60, −12)]). See Figure S3 and Table S5 in Supplement 1 for node-level results from the IQ-matched subset.

Discussion

This data-driven approach revealed widespread differences in connectivity between DYS and NI readers (Figure 2). Many

differences were in areas not previously detected by activation-based fMRI analyses, suggesting that dyslexia is a complex disorder that cannot be reduced to alterations in a small number of brain regions. Here, we discuss five themes that emerged from this whole-brain survey and subsequent node profiles. Relative to NI readers, DYS readers showed: 1) decreased connectivity along the visual pathway as well as between visual and prefrontal regions; 2) decreased lateralization of language to the left hemisphere; 3) increased connectivity to limbic regions and the default mode; 4) reduced and altered connectivity to the VWFA; and 5) persistent connectivity to a left-hemisphere anterior language region.

Connectivity Along the Visual Pathway and Between Visual Areas and Prefrontal Regions Is Disrupted in Dyslexia

Activity among nodes of the visual pathway was better synchronized in the NI group across ages. In young readers, the strength of NI network in occipital and occipitoparietal regions was notable on a whole-brain level (Figure 2A). Specifically, young NI readers showed stronger connectivity between node A in the

Table 3. Node-Level Analysis in Older Readers

Node	Region	Talairach	NI > DYS Edges	DYS > NI Edges	Sum of Edges	Diff of Edges
Nodes with a Sum of Edge Differences of at Least 10 ^a :						
J ^b	L iPL (BA7/39)	(−34, −56, 43)	4	14	18	−10
K	R calc/ling	(13, −55, 12)	9	4	13	5
L	L precuneus	(−13, −62, 25)	4	9	13	−5
M	L calc/ling	(−13, −50, 6)	12	0	12	12
N	L mTG (BA19)	(−47, −68, 5)	3	9	12	−6
O	L pCC/calc	(−10, −69, 11)	4	7	11	−3
P	L post iFG (BA44/6)	(−43, 10, 31)	6	4	10	2
Q ^b	L ant iFG (BA46/47)	(−42, 43, 8)	0	10	10	−10
Node Corresponding to the VWFA:						
R ^b	L fusiform	(−42, −60, −12)	6	3	9	3

ant, anterior; iFG, inferior frontal gyrus; iPL, inferior parietal lobule; ling., lingual gyrus; mTG, medial temporal gyrus; post, posterior; VWFA, visual word-form area; other abbreviations as in Table 2.

^aShown in Figure 2B.

^bShown in Figure 4.

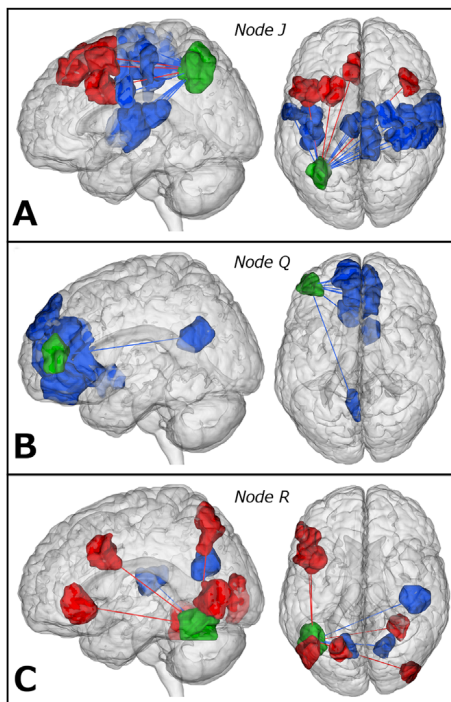


Figure 4. Visualization of connectivity profiles of selected nodes in older readers. We display the connectivity profile of three nodes with maximal group differences in connectivity (of a total of 207 nodes; see Results section 2 for how these nodes were selected). In each case the selected node is shown in green (see Table 3 for coordinates of each selected node), whereas nodes more strongly connected to the selected node in the NI > DYS (“NI”) network are shown in red, and nodes more strongly connected to the seed in the DYS > NI (“DYS”) network are shown in blue (see Table S2 in Supplement 1 for the coordinates of all NI and DYS partner nodes). Red and blue lines schematize connectivity between the selected node and each of its functional partners. Approximate anatomical locations of selected nodes: (A) left inferior parietal lobule/BA 7 (node J); (B) left anterior inferior frontal gyrus/BA 46 (node Q); and (C) left fusiform gyrus/visual word-form area (node R). Note that all figures are shown in neurological convention: subject-left is image-left, axial views are top-down, and coronal views are posterior. Abbreviations as in Figure 3.

left superior cuneus and nearby nodes in bilateral visual association cortices (Figure 3A), between node D in the right calcarine sulcus and bilateral visual association cortices (Figure 3D), and between node E in the right superior cuneus and bilateral striate and extrastriate cortices (Figure 3E). Taking functional coupling between primary visual cortex and its extrastriate partners to represent feed-forward and/or feedback activity, these results indicate that information transfer along the visual pathway follows better-formed connections in NI readers.

Furthermore, NI readers showed stronger functional connectivity between the visual pathway and prefrontal cortex (PFC). In the NI network of young readers, nodes C and E were more strongly connected to the medial PFC (Figures 3C and 3E), and in the NI network of older readers, node J in the left inferior parietal lobule was more strongly connected to the left medial PFC and bilateral superior PFC (Figure 4A). Evidence from several techniques—including fMRI (46), magnetoencephalography (47), and transcranial magnetic stimulation (48)—has shown that functional coupling between PFC and visual areas reflects top-down modulation of attention to visual stimuli. That this connectivity was stronger in NI readers suggests that they are better able to control activity in the visual pathway by focusing their attention on textual stimuli.

This role for attention systems working in concert with visual processing supports a growing body of evidence that dyslexia is, at least in part, a disorder of attention (49). Behavioral studies report impaired visual attention in individuals with dyslexia (50–52), including a reduced visual attention span (53), an impaired ability to shift attention (54), and deficits in serial search and spatial cueing (55). These deficits are general—that is, they affect DYS processing of not just text but all types of visual stimuli. However, previous fMRI studies of dyslexia have largely failed to find activation differences in primary visual and/or visual association cortices—areas where differences might be predicted, given the general nature of the behavioral deficits.

The current study helps resolve the discrepancy between behavioral results and activation-based fMRI findings: Although visual areas might not be differentially active across reading groups, they differ in the strength of their connections to one another and to other brain regions crucial for reading. In other words, the problem is not that DYS readers fail to use visual and attention regions altogether, but that they use them in different and evidently less-successful ways.

DYS Readers Are Slow to Lateralize Language to the Left Hemisphere

In most people, the left hemisphere is dominant for language (56), and language lateralization increases between 5 and 20 years of age (57). Present results show that NI readers have stronger left lateralization for language than DYS readers, who rely on bilateral systems. This extends previous findings, indicating that right-hemisphere homologs are not only more active in dyslexia but also more strongly connected to the rest of the brain.

Young NI readers showed greater connectivity from the left inferior frontal gyrus (IFG) and anterior insula to node C in left medial PFC (Figure 3C). The left IFG, which contains Broca’s area, is involved in language, including semantic, syntactic, and phonological processing (58). In typically developing readers, reading initially recruits these anterior language regions as children learn to map visual word forms to their phonological and semantic content. Our results extend these findings, suggesting that successful reading in young people depends on the synchrony of activity in left-hemisphere language regions with the ipsilateral PFC, likely reflecting modulation of attention to language stimuli.

Young DYS readers, by contrast, showed increased overall connectivity in the right hemisphere (see Figure 2A, axial view). Specifically, two nodes in the visual pathway were more strongly connected to right-hemisphere language homologs in DYS readers: node D in the right calcarine sulcus was more connected to the right IFG (Figure 3D); and node A in the left cuneus was more strongly connected to the right angular gyrus and right hippocampus/fusiform gyrus (Figure 3A). Although activity and connectivity of the angular and fusiform gyri have been associated with successful reading (18,59), this activity is also typically lateralized to the left hemisphere in NI readers. In addition, node F in the right supramarginal gyrus showed increased connectivity to nodes both ipsilateral and contralateral in the DYS network (Figure 3F).

Results from older readers indicate that, by 20 years of age, differences in lateralization have diminished but not disappeared (Figure 2B, axial view; Figure 4A). It seems, then, that DYS readers do eventually attain left-weighted language connectivity but at a slower rate—and to a lesser degree—than NI readers.

DYS Readers Show Altered Connectivity in the Posterior Cingulate Cortex/Default-Mode Network

The posterior cingulate cortex (pCC) emerged as a locus of differential connectivity in young readers (Figure 3B). Work in humans and nonhuman primates indicates that the pCC functions as a cortical hub, integrating information from distinct brain regions and networks (60). The pCC is also considered part of the default mode, or the network of regions that are active in the absence of any particular task (61). Our results show that in DYS readers, activity in the pCC is better synchronized with other areas of the default-mode network (dorsal and ventral cingulate cortices) and medial PFC, whereas in NI readers, pCC activity is better synchronized with visual association regions. Given the “hub” status of the pCC, stronger connectivity between the pCC and the dorsal visual pathway and left fusiform gyrus for the NI group (Figure 3B) could reflect better integration and cognitive control of visual information by these readers.

Because, like visual areas, the pCC and other default-mode regions have largely failed to emerge in activation-based studies of dyslexia, it seems that the functional coupling of these regions rather than their magnitude of activation separates DYS from NI readers. Future studies using data obtained in the resting state as well as during task will help clarify how activity/connectivity in these regions relate to dyslexia.

Connectivity to the VWFA Is Reduced and Altered in Older DYS Readers

The VWFA, although not differentially connected in young readers, emerged in older readers as more strongly connected in the NI group (Table 3). These results extend previous reports that, in NI readers, VWFA activity increases with age (62,63) and that its functional connectivity increases with age and reading skill into the young adult years (21). Our findings indicate that there is not yet a significant discrepancy in VWFA connectivity between dyslexic and younger good readers but that the gap widens with age as good readers reach “expert” status.

In older readers, the connections of this node in the NI network were to bilateral extrastriate cortices, left IFG, and left medial PFC (Figure 4C). These couplings could reflect successful information transfer between the VWFA and general visual association areas (extrastriate), mapping of word forms to language (IFG), and attentional modulation of this process (medial PFC), all preferentially recruiting the left hemisphere. The DYS readers showed increased connectivity between the VWFA and other bilateral visual association regions as well as to the right primary auditory cortex. Thus DYS readers do not completely fail to develop connectivity to the VWFA but rather do so in altered, perhaps compensatory circuits.

DYS Readers Show Persistent Connectivity to a Left Anterior Language Region

A striking finding among older participants was increased connectivity to the left IFG in DYS readers (node Q; Figure 4B). This node’s connections in the DYS network involved medial PFC, anterior cingulate, and left caudate. Although this area is multifunctional, many studies have attributed phonology in particular to this region (5). Its connectivity profile in older readers supports theories holding that DYS continue to rely on effortful mental articulation, or “sounding out,” strategies instead of transitioning to more rapid, visual-based systems.

Conclusions

We have presented the most comprehensive analysis of functional brain connectivity in dyslexic versus nonimpaired readers to

date. Of the approximately 20,000 connections investigated in each dataset, a small but impressive fraction showed highly significant differences in functional connectivity between groups, suggesting that dyslexia is not simply attributable to dysfunction in a few specific language nodes. These data-driven, whole-brain results deepen and extend what was known from activation-based fMRI studies about the neural underpinnings of dyslexia.

We thank Daniel Geschwind and four anonymous reviewers for their thoughtful critiques of the manuscript. EF is supported by a Gruber Science Fellowship from the Gruber Foundation via Yale University. This work was supported in part by NIH grant EB009666 to RTC.

The authors report no biomedical financial interests or potential conflicts of interest.

Supplementary material cited in this article is available online at <http://dx.doi.org/10.1016/j.biopsych.2013.08.031>.

1. Lyon GR, Shaywitz SE, Shaywitz BA (2003): A definition of dyslexia. *Ann Dyslexia* 53:1–14.
2. Interagency Committee on Learning Disabilities (1987): *Learning Disabilities: A Report to the U.S. Congress*. Washington, DC: US Government Printing Office.
3. Shaywitz SE, Fletcher J, Shaywitz BA (1994): Issues in the definition and classification of attention deficit disorder. *Top Lang Disord* 14: 1–25.
4. Shaywitz SE (2003): *Overcoming Dyslexia: A New and Complete Science-Based Program for Reading Problems at Any Level*. New York: Alfred A. Knopf.
5. Shaywitz BA, Shaywitz SE, Pugh KR, Mencl WE, Fulbright RK, Skudlarski P, *et al.* (2002): Disruption of posterior brain systems for reading in children with developmental dyslexia. *Biol Psychiatry* 52: 101–110.
6. Brambati SM, Termine C, Ruffino M, Danna M, Lanzi G (2006): Neuropsychological deficits and neural dysfunction in familial dyslexia. *Brain Res* 1113:174–185.
7. Kronbichler M, Hutzler F, Staffen W, Mair A (2006): Evidence for a dysfunction of left posterior reading areas in German dyslexic readers. *Neuropsychologia* 44:1822–1832.
8. Cohen L, Dehaene S, Naccache L, Lehéricy S, Dehaene-Lambertz G, Hénaff MA, Michel F (2000): The visual word form area: Spatial and temporal characterization of an initial stage of reading in normal subjects and posterior split-brain patients. *Brain* 123: 291–307.
9. Cohen L, Dehaene S (2004): Specialization within the ventral stream: The case for the visual word form area. *Neuroimage* 22:466–476.
10. Dehaene S, Cohen L, Sigman M, Vinckier F (2005): The neural code for written words: A proposal. *Trends Cogn Sci* 9:335–341.
11. Vinckier F, Dehaene S, Jobert A, Dubus JP, Sigman M, Cohen L (2007): Hierarchical coding of letter strings in the ventral stream: Dissecting the inner organization of the visual word-form system. *Neuron* 55: 143–156.
12. Price CJ, Devlin T (2011): The interactive account of ventral occipito-temporal contributions to reading. *Trends Cogn Sci* 15:246–253.
13. Price CJ, Mechelli A (2005): Reading and reading disturbance. *Curr Opin Neurobiol* 15:231–238.
14. Shaywitz SE, Shaywitz BA (2005): Dyslexia (specific reading disability). *Biol Psychiatry* 57:1301–1309.
15. Richlan F, Kronbichler M, Wimmer H (2011): Meta-analyzing brain dysfunctions in dyslexic children and adults. *Neuroimage* 56: 1735–1742.
16. Richlan F (2012): Developmental dyslexia: Dysfunction of a left hemisphere reading network. *Front Hum Neurosci* 6:1–5.
17. Van den Heuvel MP, Hulshoff Pol HE (2010): Exploring the brain network: A review on resting-state fMRI functional connectivity. *Eur Neuropsychopharmacol* 20:519–534.
18. Horwitz B, Rumsey JM, Donohue BC (1998): Functional connectivity of the angular gyrus in normal reading and dyslexia. *Proc Natl Acad Sci U S A* 95:8939–8944.

19. Stanberry LI, Richards TL, Berninger VW, Nandy RR, Aylward EH, Maravilla KR, *et al.* (2006): Low-frequency signal changes reflect differences in functional connectivity between good readers and dyslexics during continuous phoneme mapping. *Magn Reson Imaging* 24:217–229.
20. Van der Mark S, Klaver P, Bucher K, Maurer U (2011): The left occipitotemporal system in reading: Disruption of focal fMRI connectivity to left inferior frontal and inferior parietal language areas in children with dyslexia. *Neuroimage* 54:2426–2436.
21. Vogel AC, Miezin FM, Petersen SE, Schlaggar BL (2012): The putative visual word form area is functionally connected to the dorsal attention network. *Cereb Cortex* 22:537–549.
22. Koyama MS, Di Martino A, Kelly C, Jutagir DR, Sunshine J, Schwartz SJ, *et al.* (2013): Cortical signatures of dyslexia and remediation: An intrinsic functional connectivity approach. *PLoS One* 8:e55454.
23. Shen X, Papademetris X, Constable RT (2010): Graph-theory based parcellation of functional subunits in the brain from resting-state fMRI data. *Neuroimage* 50:1027–1035.
24. Shen X, Tokoglu F, Papademetris X, Constable RT (2013): Groupwise whole-brain parcellation from resting-state fMRI data for network node identification. *Neuroimage* 82:403–415.
25. Wiederholt JL, Bryant BR (1992): *Gray Oral Reading Tests, 3rd ed.* Austin, TX: Pro-Ed.
26. Torgesen JK, Wagner RK, Rashotte CA (1999): *Test of Word Reading Efficiency (TOWRE)*. Austin, TX: Pro-Ed.
27. Woodcock RW, Johnson MB (1989): *Woodcock-Johnson Psycho-Educational Battery-Revised*. Allen, TX: Developmental Learning Materials.
28. Germano E, Gagliano A, Curatolo P (2010): Comorbidity of ADHD and dyslexia. *Dev Neuropsychol* 35:475–493.
29. Wechsler D (1991): *Wechsler Intelligence Scale for Children, 3rd ed.* San Antonio, TX: Psychological Corporation.
30. Ferrer E, McArdle JJ, Shaywitz BA, Holahan JM, Marchione K, Shaywitz SE (2007): Longitudinal models of developmental dynamics between reading and cognition from childhood to adolescence. *Dev Psychol* 43:1460–1473.
31. Siegel LS (1988): Evidence that IQ scores are irrelevant to the definition and analysis of reading disability. *Can J Psychol* 43:201–215.
32. Jones TB, Bandettini PA, Kenworthy L, Case LK, Milleville SC, Martin A, Birm RM (2010): Sources of group differences in functional connectivity: An investigation applied to autism spectrum disorder. *Neuroimage* 49:401–414.
33. Zalesky A, Fornito A, Bullmore ET (2010): Network-based statistic: Identifying differences in brain networks. *Neuroimage* 53:1197–1207.
34. Fornito A, Zalesky A, Bullmore ET (2010): Network scaling effects in graph analytic studies of human resting-state fMRI data. *Front Syst Neurosci* 4:22.
35. Tzourio-Mazoyer N, Landeau B, Papathanassiou D, Crivello F, Etard O, Delcroix N, *et al.* (2002): Automated anatomical labeling of activations in SPM using a macroscopic anatomical parcellation of the MNI MRI single-subject brain. *Neuroimage* 15:273–289.
36. Liu Y, Liang M, Zhou Y, He Y, Hao Y, Song M, *et al.* (2008): Disrupted small-world networks in schizophrenia. *Brain* 131:945–961.
37. Supekar K, Menon V, Rubin D, Musen M, Greicius MD (2008): Network analysis of intrinsic functional brain connectivity in Alzheimer's disease. *PLoS Comput Biol* 4:e1000100.
38. Lynall M-E, Bassett DS, Kerwin R, McKenna PJ, Kitzbichler M, Muller U, Bullmore E (2010): Functional connectivity and brain networks in schizophrenia. *J Neurosci* 30:9477–9487.
39. Van den Heuvel MP, Mandl RCW, Stam CJ, Kahn RS, Hulshoff Pol HE (2010): Aberrant frontal and temporal complex network structure in schizophrenia: A graph theoretical analysis. *J Neurosci* 30:15915–15926.
40. Fair DA, Dosenbach NUF, Church JA, Cohen AL, Brahmbhatt S, Miezin FM, *et al.* (2007): Development of distinct control networks through segregation and integration. *Proc Natl Acad Sci U S A* 104:13507–13512.
41. Stevens AA, Tappan SC, Garg A, Fair DA (2012): Functional brain network modularity captures inter- and intra-individual variation in working memory capacity. *PLoS One* 7:e30468.
42. Van den Heuvel MP, Mandl RCW, Kahn RS, Hulshoff Pol HE (2009): Functionally linked resting-state networks reflect the underlying structural connectivity architecture of the human brain. *Hum Brain Mapp* 30:3127–3141.
43. Martuzzi R, Ramani R, Qiu M, Shen X, Papademetris X, Constable RT (2011): A whole-brain voxel based measure of intrinsic connectivity contrast reveals local changes in tissue connectivity with anesthetic without a priori assumptions on thresholds or regions of interest. *Neuroimage* 58:1044–1050.
44. Alexander-Bloch A, Lambiotte R, Roberts B, Giedd J, Gogtay N, Bullmore E (2010): The discovery of population differences in network community structure: New methods and applications to brain functional networks in schizophrenia. *Neuroimage* 59:3889–3900.
45. Holmes CJ, Hoge R, Collins L, Woods R, Toga AW, Evans AC (1998): Enhancement of MR images using registration for signal averaging. *J Comput Assist* 22:324–333.
46. Gazzaley A, Rissman J, Cooney J, Rutman A, Seibert T, Clapp W, D'Esposito M (2007): Functional interactions between prefrontal and visual association cortex contribute to top-down modulation of visual processing. *Cereb Cortex* 17:i125–135.
47. Siegel M, Donner TH, Oostenveld R, Fries P, Engel AK (2008): Neuronal synchronization along the dorsal visual pathway reflects the focus of spatial attention. *Neuron* 60:709–719.
48. Zanto TP, Rubens MT, Thangavel A, Gazzaley A (2011): Causal role of the prefrontal cortex in top-down modulation of visual processing and working memory. *Nat Neurosci* 14:656–661.
49. Shaywitz SE, Shaywitz BA (2008): Paying attention to reading: the neurobiology of reading and dyslexia. *Dev Psychopathol* 20:1329–1349.
50. Valdois S, Bosse M-L, Tainturier M-J (2004): The cognitive deficits responsible for developmental dyslexia: Review of evidence for a selective visual attentional disorder. *Dyslexia* 10:339–363.
51. Vidyasagar TR, Pammer K (2010): Dyslexia: A deficit in visuo-spatial attention, not in phonological processing. *Trends Cogn Sci* 14:57–63.
52. Gabrieli JDE, Norton ES (2012): Reading abilities: Importance of visual-spatial attention. *Curr Biol* 22:R298–R299.
53. Bosse ML, Tainturier MJ, Valdois S (2007): Developmental dyslexia: The visual attention span deficit hypothesis. *Cognition* 104:198–230.
54. Facoetti A, Paganoni P, Turatto M, Marzola V, Mascetti GG (2000): Visual-spatial attention in developmental dyslexia. *Cortex* 36:109–123.
55. Franceschini S, Gori S, Ruffino M, Pedrolli K, Facoetti A (2012): A causal link between visual spatial attention and reading acquisition. *Curr Biol* 22:814–819.
56. Knecht S, Deppe M, Dräger B, Bobe L, Lohmann H, Ringelstein E-B, Henningsen H (2000): Language lateralization in healthy right-handers. *Brain* 123:74–81.
57. Szafarski JP, Holland SK, Schmithorst VJ, Byars AW (2006): fMRI study of language lateralization in children and adults. *Hum Brain Mapp* 27:202–212.
58. Price CJ (2012): A review and synthesis of the first 20 years of PET and fMRI studies of heard speech, spoken language and reading. *Neuroimage* 62:816–847.
59. Hampson M, Tokoglu F, Sun Z, Schafer RJ, Skudlarski P, Gore JC, Constable RT (2006): Connectivity-behavior analysis reveals that functional connectivity between left BA39 and Broca's area varies with reading ability. *Neuroimage* 31:513–519.
60. Leech R, Braga R, Sharp DJ (2012): Echoes of the brain within the posterior cingulate cortex. *J Neurosci* 32:215–222.
61. Raichle ME, Macleod AM, Snyder AZ, Powers WJ, Gusnard DA, Shulman GL (2001): A default mode of brain function. *Proc Natl Acad Sci U S A* 98:676–682.
62. Booth JR, Burman DD, Van Santen FW, Harasaki Y, Gitelman DR, Parrish TB (2001): The development of specialized brain systems in reading and oral language. *Child Neuropsychol* 7:119–141.
63. Shaywitz BA, Skudlarski P, Holahan JM, Marchione KE, Constable RT, Fulbright RK, *et al.* (2007): Age-related changes in reading systems of dyslexic children. *Ann Neurol* 61:363–370.